Journal of Analytical and Applied Pyrolysis 109 (2014) 249–257

Contents lists available at ScienceDirect

Journal of Analytical and Applied Pyrolysis

journal homepage: www.elsevier.com/locate/jaap

Detailed compositional analysis and structural investigation of a bio-oil from microwave pyrolysis of kraft lignin

Sherif Farag[a], Dongbao Fu[b], Philip G. Jessop[b], Jamal Chaouki[a,*]

[a] Research Center In Process Engineering-Biorefinery (CRIP), Department of Chemical Engineering, Ecole Polytechnique Montreal, P.O. Box 6079, Station Centre-ville, Montréal, QC, Canada H3C 3A7

[b] Department of Chemistry, Queen's University, 90 Bader Lane, Kingston, Ontario K7L 3N6, Canada

ARTICLE INFO

Article history:
Received 22 March 2014
Accepted 13 June 2014
Available online 19 June 2014

Keywords:
Microwave pyrolysis
Kraft lignin
Pyrolysis oil
^{31}P NMR
^{13}C NMR
GC–MS

ABSTRACT

This work investigates composition and structure of a bio-oil produced form microwave pyrolysis of kraft lignin at different conditions. The studied variables were content of microwave-absorber (20–40 wt%) and nominal setting power (1.5–2.7 kW). The measured temperatures after applying the selected conditions for 800 s were 900, 980, 1065, 1150, and 1240 K. The obtained yields of the aqueous phase, oil phase, non-condensable gas, and solid were 17–21%, 15–20%, 21–27%, and 32–40%, respectively. To investigate the extracted chemicals quantitatively and qualitatively, GC–MS and GC–FID were performed on the liquid samples. In addition, ^{31}P and ^{13}C NMR spectroscopy were implemented to provide detailed structure information for the whole oil phase and the raw material. Furthermore, different degradation pathways were suggested to represent the thermal-decomposition of lignin bonds.

1. Introduction

Recently, biomass has been employed as a renewable resource of value-added bio-chemicals. Developing bio-chemicals is one opportunity for dealing with the unexpected challenges that have faced the forest industry in North America for the past few years, such as decreasing demand and competition with low cost sources of wood. As well, generating energy from biomass is one way to compensate for the rapid increase in energy demand expected in the next few years.

Lignocellulosic biomass is composed of three intertwined components: cellulose, hemicellulose, and lignin. The dry basis weight of each is 35–45%, 25–30%, and 20–35%, respectively [1–3]. This distribution depends on the species, the environment in which it was grown, and other factors. Lignin is recognized to result from the polymerization of three aromatic alcohols: *p*-coumaryl, coniferyl, and sinapyl alcohol, as depicted in Fig. 1 [1,3,4].

Even though lignin is the only renewable source of aromatics in nature and the third-most abundant natural polymer after cellulose and hemicellulose, it has received less attention in research than the other biomass components. In addition, the annual production of lignin in the US paper industry is over 50 million tons, yet only 2% of this material is converted to bio-products, whereas the rest is combusted to recover energy and chemicals Farag et al. [5].

Lignin can be converted into chemicals and/or energy using chemical, biological, or physical technology. One of the techniques applied in thermal technology is pyrolysis. Pyrolysis is a thermal decomposition of chemical bonds by supplying heat energy in an oxygen-free environment. The main pyrolysis products are: (1) solid, mostly carbon, which can be used as a solid fuel, soil additive, and other applications. (2) Condensable gas, which is a potential source for value added chemicals that could replace petrochemicals; and (3) non-condensable gas [1,6]. The needed heat energy for pyrolysis can be provided by heat transfer from a heating source. Otherwise, it can be generated within the heated material by an electromagnetic exposure (microwave heating). This pyrolysis is called "microwave pyrolysis" (MW-P).

Microwave heating (MWH) is a volumetric energy conversion mechanism within the target material rather than superficial heat transfer as in conventional heating (CH). MWH has been established in different sectors as it can eliminate several issues/limitations in contrast to CH such as formation of a temperature gradient inside and outside the heated material, and char layer formation of pyrolysis material. Furthermore, it has been demonstrated that a desired temperature gradient and/or hot or cold spots can be generated within the payload in a simple way, compared to CH [7]. Further details regarding MWH can be found in Farag et al. [7].

* Corresponding author. Tel.: +1 514 340 4711x4034; fax: +1 514 340 4159.
E-mail address: jamal.chaouki@polymtl.ca (J. Chaouki).

http://dx.doi.org/10.1016/j.jaap.2014.06.005
0165-2370/

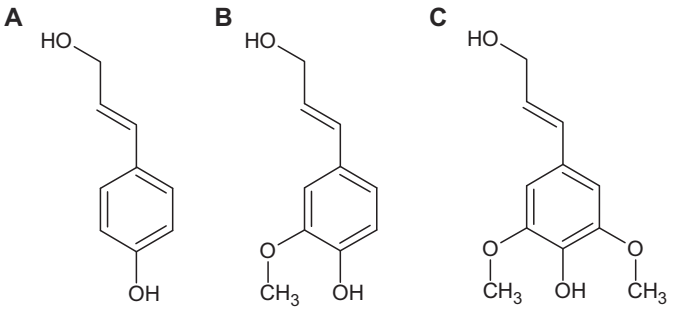

Fig. 1. The three monolignols of a lignin network: (A) coumaryl alcohol, (B) coniferyl alcohol, and (C) sinapyl alcohol.

Pyrolysis of lignin and characterization of the liquid product have been investigated over the past two decades. Zheng et al. [8] have examined fast pyrolysis of lignin under the catalytic effect of $Mo_2N/\gamma\text{-}Al_2O_3$, using a pyrolysis–gas chromatography/mass spectrometry system (Py–GC–MS). The same analytical technique was used by Lou et al. [9] to study the effect of temperature and catalysts (sodium chloride, permutite) on the pyrolysis of bamboo lignin and Jiang et al. [10] to discuss the temperature dependence of the composition of lignin pyrolysis products. Choi and Meier [11] investigated the pyrolysis of kraft lignin under the effect of different temperatures and catalysts (Zeolite HZSM-5, FCC and Olivine), employing GC–MS/GC–FID to analyze the liquid product. Py–GC–MS and TGA/FTIR were used by Zhang et al. [12], to study the pyrolysis of three lignin types: prairie cord grass, aspen, and synthetic kraft lignin. De Wild et al. [1] examined the pyrolyis of lignin from two different biomass sources using a fluidized bed reactor, employing GC–MS to analyze the liquid product. Luo et al. [13] have discussed the thermal behavior of organosolv lignin under the catalytic effect of zeolites, using TGA-FTIR.

As has been shown, most of the previous work has been done by employing GC–MS and/or FT-IR to analyze the obtained liquid. Nevertheless, the complexity of the pyrolysis crude liquid limits the use of these instruments due to different issues and consequently many chemical components could not be identified. Therefore, the main goal of the present study was to investigate the structures of kraft lignin pyrolysis liquids under different MW-P conditions. This was accomplished using quantitative NMR to analyze the liquid products and the raw material as it can provide detailed structural information. Such investigations improve understanding about MW-P mechanisms, which leads to more control in the degradation pathways.

2. Experimental work

2.1. Raw material

The raw material used in this work was softwood kraft lignin supplied by FPInnovations, Pointe-Claire, Quebec, Canada. It was precipitated from a Canadian kraft mill using The LignoForce System, a patent-pending process that was developed by FPInnovations and licensed to NORAM Engineers and Constructors, Vancouver, British Columbia, Canada, for commercialization.

Lignin was characterized via CHNS analysis: C = 63.27%, H = 5.79%, N = 0.07%, and S = 1.56%, and proximate analysis: fixed carbon = 37%, volatiles = 62%, and ash = 1%. In addition, it was analyzed using quantitative ^{13}C NMR and ^{31}P NMR spectroscopy as will be shown later.

Indeed, lignin does not interact well with electromagnetic waves (EMW). Therefore, it was homogeneously mixed with a good microwave-to-heat convertor, the solid product after MW-P of kraft lignin, which is a strong microwave-to-heat convertor [14-16]. If char is absent, the extracted product is expelled from the lignin particles, forming an exceedingly sticky material. Finally, after cooling, the formed material converts into a very strong block, which is extremely difficult to break down [5].

Table 1
The coded vales and the corresponding actual values and final temperatures applied in MW-P of kraft lignin.

Run #	Coded value		Actual value		Final temperature [K]
	Char wt%	Nominal Power	Char wt%	Nominal power [kW]	
1	−1	−1	20	1.5	900
2	−1	1	20	2.7	980
3	0	0	30	2.1	1065
4	1	−1	40	1.5	1150
5	1	1	40	2.7	1240

2.2. Experimental design

To study the effect of MW-P conditions on product distribution and crude liquid structure, a central composite experimental design method was applied. This method gave the optimal number of experiments as well as the conditions of each. In this work, two independent parameters were chosen (A_i): (1) the concentration of a MW-thermal-catalyst (A_1 [wt%]) with $A_{1,min} = 20$ and $A_{1,max} = 40$ in the total initial mass (lignin + char) and (2) the MW-nominal setting power (A_2 [kW]) with $A_{2,min} = 1.5$ and $A_{2,max} = 2.7$. The variables A_i were coded as a_i according to Eq. (1).

$$a_i = \frac{A_i - A_o}{\Delta A} \quad (1)$$

where a_i is a dimensionless coded value, A_i is the real value of an independent variable, and A_o is the real value of the independent variable at the center point (0,0). ΔA is the step change, which equals 10 for the first parameter and 0.6 for the second one. Table 1 shows the coded and actual values for the independent parameters. In order to guarantee the reproducibility, each experiment was repeated three times, and the average value was represented as will be shown later.

2.3. Experimental setup

The experimental work was carried out in a bench scale Microwave-oven (MW-O) (Microwave Research Inc; Model: BP-211, 230 V, 2.45 GHz, and setting power up to 3.2 kW). The oven cavity has inner dimensions of 510 × 250 × 320 mm. As electronic devices are highly affected by the surrounding temperature, an alumina box (muffle) with the dimensions of 390 × 180 × 170 mm was kept inside the oven cavity during the heating. This muffle protects the oven's electronic devices from most of the emitted heat and unwanted/unexpected explosions, or combustion during MW-P. A quartz semi-batch cylinder reactor with the dimensions of ID: 70 mm and L: 250 mm was used after connecting it to a condensation system to collect the condensable gas while the non-condensable gas passes directly through, as shown in Fig. 2.

The employed condensation system consists of a set of vertical metallic tubes. These tubes were connected in series at one end while the other ends were connected via a 500 mL two neck Pyrex flask. The reactor outlet was connected to the condensation system via a metallic connection. This connection was kept at 200 °C, to avoid any condensation before the freezing zone.

Temperature measurement was done using the innovated thermometer that was used in Farag and Chaouki [17]; refer to that

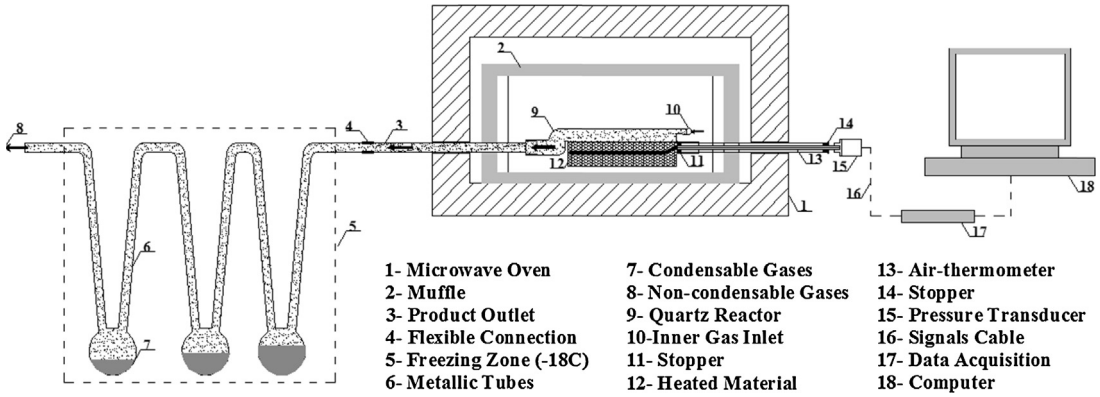

Fig. 2. The experimental set-up.

paper for a detailed description, calibration, and validation of this thermometer. Fig. 3 shows the transient mean temperatures within kraft lignin at two different concentrations of char, 20 and 40 wt%, and one nominal setting power, 2.7 kW. In this work, since MW-P was done at non-isothermal conditions, the presented temperatures are the final ones, which were reached at the end of the heating period, 800 s.

2.4. Experimental method

The procedures of each experiment were as follows. First, a constant initial mass of 300 g (char: x wt% + lignin: $(1-x)$ wt%) was carefully placed in the reactor. Afterward, the reactor was inserted inside the MW-O cavity and then connected for temperature measurement, to the inert gas inlet, and the product outlet, as illustrated in Fig. 2. Secondly, the whole system was purged in the beginning by an inert gas (N_2); furthermore, N_2 was kept during the pyrolysis with 500 mL/min of flow rate. A nominal setting power, according to Table 1, was adjusted and held for 800 s, which is the microwave exposure time for each experiment.

In the meantime, for each experiment the condensable liquid was condensed within the freezing zone, whereas the non-condensable gas passed directly through. After each experiment, the solid product was collected and weighed as soon as it cooled to ambient temperature. The same approach was used for the liquid product. The mass of non-condensable gas was calculated by subtracting the liquid and solid masses from the initial lignin mass ($(1-x)$ times the total initial mass). The collected liquid mixture was separated into two phases: (1) an oil phase, and (2) an aqueous phase which is less dense than the oil phase.

The oil and aqueous phases were analyzed using GC–MS (PerkinElmer Clarus 680 Gas Chromatograph and a PerkinElmer Clarus 600T Mass Spectrometer), GC–FID (Shimadzu GC-17 A), quantitative ^{31}P and ^{13}C NMR spectroscopy (Bruker Avance 500 MHz NMR spectrometer). The detailed methods of these analyses were reported by Fu et al. [18] and therefore will not be presented here. Water content of each sample was determined by Karl–Fischer Titration using a Mettler Toledo C20 Coulometric KF Titrator. These analyses and measurements (GC–MS, GC–FID, ^{13}C NMR, ^{31}P NMR, and water content) were done on a mix of three samples produced via three repetitions at the same conditions.

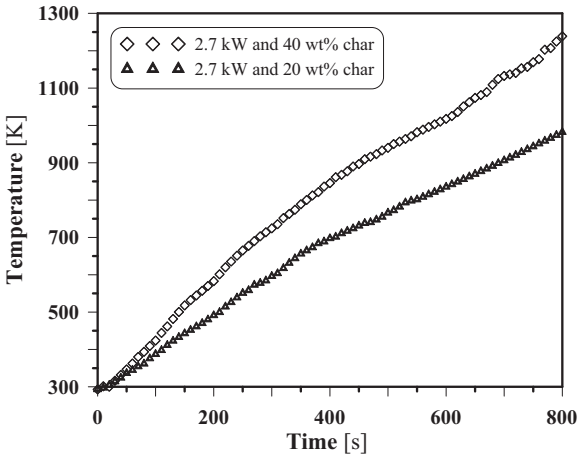

Fig. 3. The transient mean temperature of MW-P of kraft lignin at two various conditions.

3. Results and discussion

3.1. Products distribution

The power setting and char wt% that were used at each run produced a specific heating rate and therefore a specific final temperature. A comparison made between two runs having the same nominal power setting but different concentrations of char demonstrated that char concentration had a greater effect on the final temperature than the nominal power setting. For instance, when the concentration of char was changed from 20% to 40% at 1.5 kW, the final temperature was increased by 250 °C. On the other hand, when the power setting was changed from 1.5 kW to 2.7 kW at 20% of char concentration, the final temperature was increased by 80 °C. This means the same heating rate can be obtained at a lower power setting by raising the char concentration. However, char concentration should be optimized in order to prevent an adverse effect on the product distribution and quality.

Fig. 4 shows the yields of each product for the conditions under investigation. These yields were calculated based on the initial mass dry basis. The presented values are the average of three repetitions under the same conditions, and the presented error bars are their standard deviations. The maximum standard deviation was ±2 for all products except for the aqueous phase, it was ±1.

The average solid yield (based on all the experiments) was 40 ± 1.8 wt% at 95% of confidence interval. In pyrolysis; generally speaking, such small variations cannot be considered to document a strong scientific explanation, because it might be an experimental error. In this work, therefore, we did not discuss the obtained solid product, instead we kept the main goal is to investigate the oil phase.

As shown in Fig. 4, increasing the final temperature increased the total liquid product. For example, when the temperature was changed from 900 K to 1240 K, the total liquid yield was increased

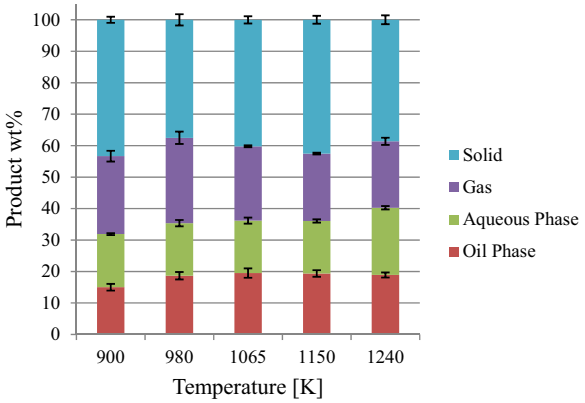

Fig. 4. The product distribution for the conditions under investigation.

from 32 wt% to 40 wt%. The same trend has been reported by Choi and Meier [11]. However, this result could be either beneficial or problematic depending on the structure of the obtained liquid and the yield of the desired chemicals.

Together Fig. 4 and Table 2, although the liquids produced at 1065 K and 1150 K have almost the same yield, the one produced at 1150 K has 12 wt% more organic compounds (in other words, 12 wt% less water content) in the aqueous phase than did the one at 1065 K. The liquid produced at 980 K, which has the maximum water content in the oil phase, has almost the same total oil wt% as the one at 1065 K. This means, if another consideration is applied (e.g. solid/gas yield, or product quality) another condition can be the best. For this reason, we chose to focus not only on quantitative but also on qualitative characterization of the liquids. Consequently, different analyses were applied on the liquid product to achieve an investigation that is based on the composition of the obtained liquid, not only based on the obtained quantity of liquid.

3.2. GC–MS and GC–FID analyses

Simply obtaining a high yield of oil is insufficient; it is important to know and to be able to optimize the composition of the oil. The liquid product was analyzed using GC–MS and GC–FID, for characterizing the extracted chemical compounds via MW-P of lignin. Table 3 lists the 42 organic compounds that were identified and quantified in the oil and aqueous phases.

Because the chemical structure of lignin is largely aromatic, all the identified compounds are aromatics as well. The identified chemical compounds in the oil and aqueous phases are presented in five groups: benzenes, phenols, guaiacols, catechols, and others. The aqueous phase contained so little organic content that identified organic compounds totalled only 15–38 mg/g in the aqueous phase; in contrast, 264–353 mg/g were found in the oil phase. Consequently, the remainder of this work will focus on the oil phase only.

The most abundant group of compounds in the oil phase was the guaiacols, which were found in a concentration range of 135–184 mg/g. Phenols were found at 74–108 mg/g while catechols were found within 31–50 mg/g. Other identified chemical compounds were collectively found in a concentration of 6–15 mg/g.

In general, the maximum concentration of the total identified compounds (353 mg/g of oil phase) was found at 1150 K. The maximum concentration of guaiacols and catechols was produced at 1150 K. On the other hand, the maximum concentration of phenols and others was found at 1065 K. The maximum concentration of benzenes was at 900 K. However, there was a concentration from 490 mg/g to 616 mg/g (calculated by subtracting 100 from the identified compounds concentration and the measured water content) in the oil phase of compounds, probably higher molecular weight compounds that could not be identified using GC–MS. Therefore, GC–MS analysis is inadequate to fully describe the composition.

Table 2
The measured water content in the aqueous and oil phases at every run.

Run #	Temp [K]	Water content [wt%]			
		Aqueous phase	Oil phase	Total liquid	Relative to initial mass
1	900	91	10	53	17
2	980	76	21	47	17
3	1065	90	14	49	18
4	1150	78	14	44	16
5	1240	73	12	44	18

3.3. Quantitative ^{31}P NMR analyses

Quantitative ^{13}P NMR spectroscopy was used to further characterize the oil phase as well as the raw material, in a total of six samples. The quantitative ^{31}P NMR spectra were acquired after in situ derivatization with 2-chloro-4,4,5,5-tetramethyl-1,3,2-dioxaphospholane (TMDP) to measure the hydroxyl groups' contents in the samples; this method was developed by Granata and Argyropoulos [19]. Fig. 5 depicts the ^{31}P NMR spectra for oil phase produced at the conditions of 40 wt% of char and 1.5 kW of nominal power. Table 4 summarizes the integration for the analyzed samples, five oils produced at the selected conditions, and the 6th for the raw material.

As shown in Table 4, the concentration of aliphatic and C5 substituted/condensed phenolic hydroxyl groups in the oil phase is lower than that in the raw material. On the other hand, each of the oil samples contained a higher concentration of guaiacyl, *p*-hydroxyphenyl, and catechol hydroxyl groups after MW-P than in the raw material.

The decrease in concentration of the aliphatic hydroxyl group is so considerable that it indicates most of the raw-material side chain hydroxyl groups were swiftly decomposed during the MW-P. The decomposition of these side chains might be attributed to form water and/or unsaturated sites, according to the pathway illustrated in Fig. 6A. On average, the concentration of aliphatic hydroxyl groups decreased by about 90% during the pyrolysis, possibly suggesting the source of the formation of water during MW-P of lignin. In fact, this is in agreement with the prior investigations; Farag et al. [5] reported that the activation energy of the obtained water is lower than that of the produced oil phase, because the water is mostly formed by the cleavage of the lignin site chain aliphatic hydroxyl groups.

The possibility of creating water by means of the decomposition of the carboxyl group is minute as the concentration of carboxyl groups in the raw material is minimal compared to the concentration of aliphatic hydroxyl groups. Therefore, the decomposition of the carboxyl group is more likely to be the source for the creation of carbon dioxide and/or unsaturated sites during the pyrolysis, as shown in Fig. 6B. As a result, the level of water measured in the total liquid product corresponds mostly to the decomposition of the side chain aliphatic hydroxyl group.

The decreased concentrations of C5 substituted/condensed phenolic hydroxyl groups in the oil phase after MW-P may be attributed to an increase in the concentrations of guaiacyl, *p*-hydroxyphenyl, and catechol hydroxyl groups, asillustrated in Fig. 7. Fig. 7 demonstrates the possible decomposition pathways for the β-5 bond, the 4-O-5 bond, and the 5-5 bond.

Comparing the increases in the concentrations of guaiacyl (up to 2-fold increase), 4-hydroxyphenyl (up to 3-fold), and catechol hydroxyl groups (up to 5-fold) shows that the increase in the catechol hydroxyl group is significantly greater than the increase in

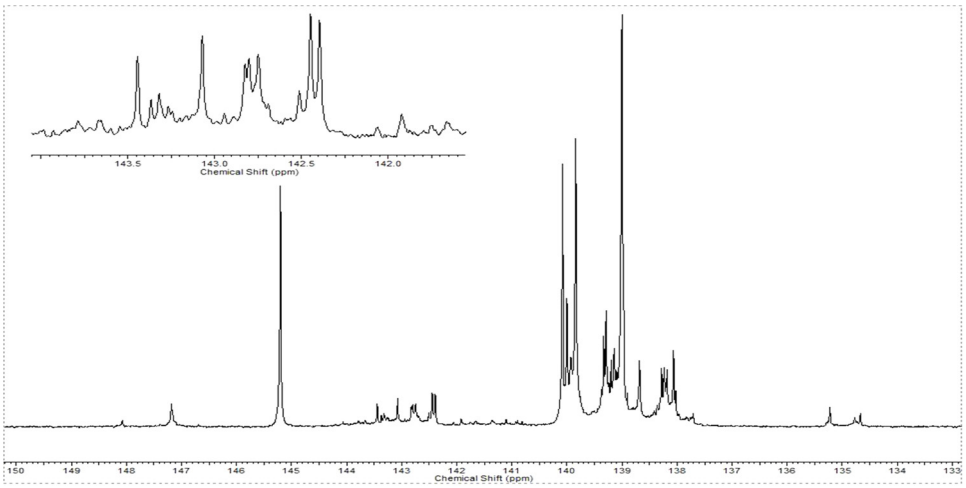

Fig. 5. Quantitative ^{31}P NMR spectrum for the oil phase obtained at the conditions of 40 wt% of char and 1.5 kW of nominal power.

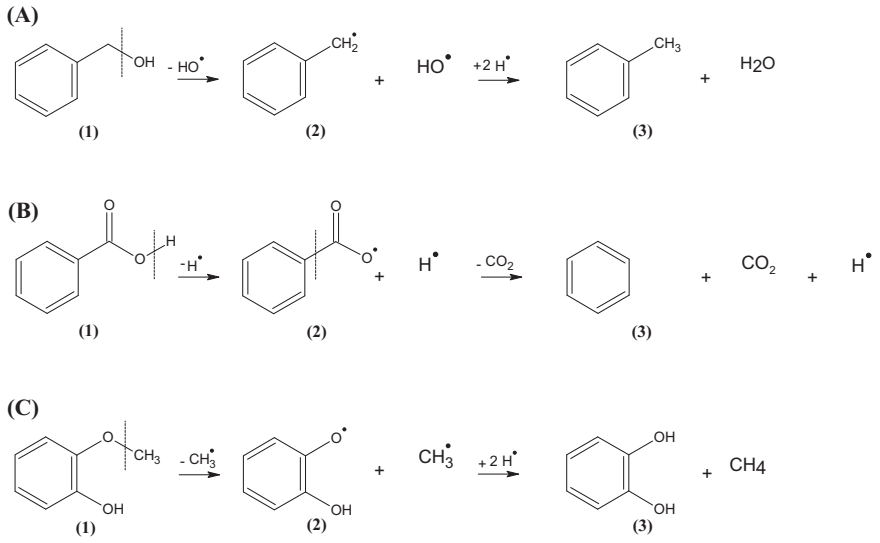

Fig. 6. Possible degradation pathways for: (A) aliphatic hydroxyl group, (B) carboxyl acid, and (3) guaiacyl hydroxyl groups.

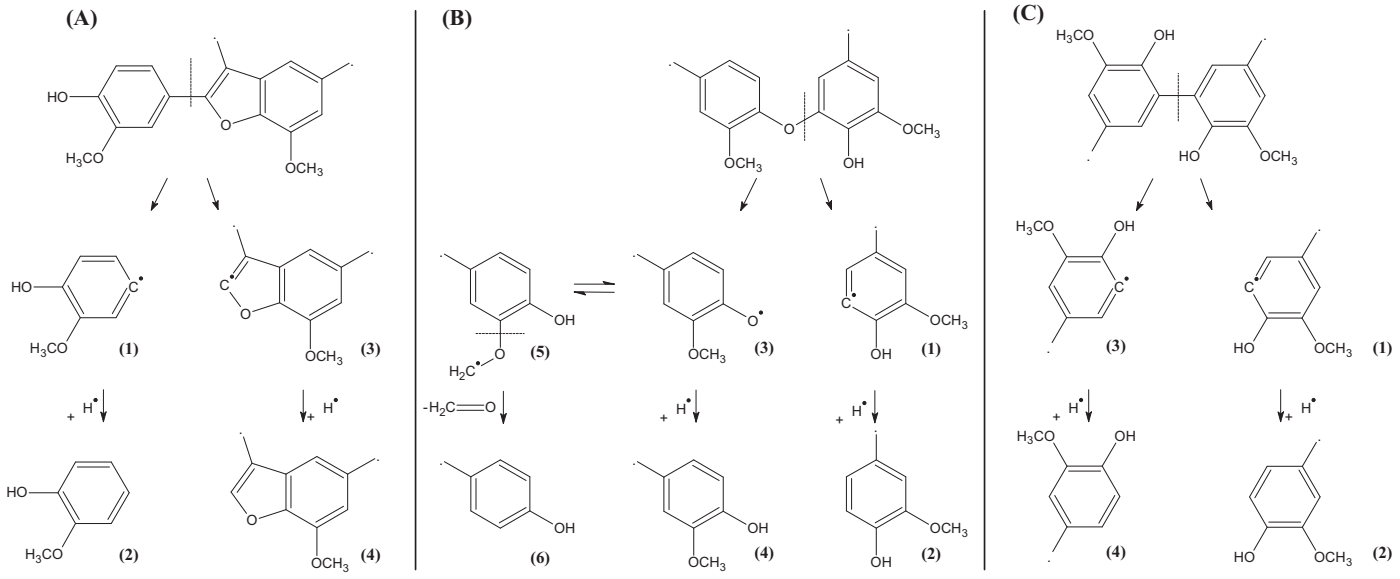

Fig. 7. Possible degradation pathways of C5 substituted/condensed phenolic hydroxyl group: (A) β-5, (B) 4-O-5, and (C) 5–5.

Table 3
Identified chemical components in the oil and aqueous phases obtained after MWP of kraft lignin.

#	RT [min]	Identification by GC–MS	Oil phase [mg/g oil phase]					Aqueous phase [mg/g aqueous phase]				
			900 K	980 K	1065 K	1150 K	1240 K	900 K	980 K	1065 K	1150 K	1240 K
		Benzenes	17.7	16.5	14.2	14.0	10.6	0.2	0.2	0.2	0.2	0.0
1	3.38	Toluene	8.1	7.2	5.3	6.4	4.5	0.2	0.2	0.2	0.2	nd
2	6.44	Styrene	3.8	3.3	2.9	1.7	1.5	nd	nd	nd	nd	nd
3	9.90	*m*-Methylstyrene	2.4	2.6	2.1	1.3	1.3	nd	nd	nd	nd	nd
4	21.46	4-Ethyl-1,2-dimethoxybenzene	1.3	1.3	1.5	1.9	1.2	nd	nd	nd	nd	nd
5	22.50	1,4-Dimethoxy 2,3-dimethylbenzene	2.1	2.1	2.4	2.7	2.1	nd	nd	nd	nd	nd
		Phenols	102.5	103.4	108.0	97.7	73.9	5.1	8.5	5.5	4.2	1.5
6	9.46	Phenol	10.3	11.5	10.8	9.6	7.7	2.4	2.7	2.4	1.9	0.7
7	12.06	*o*-Methylphenol	9.3	8.8	9.2	8.9	7.1	0.9	1.1	0.9	0.8	0.3
8	12.86	*p*-Methylphenol	12.6	11.9	12.4	11.3	nd	1.2	1.5	1.1	0.9	0.3
9	13.94	2,6-Dimethylphenol	4.9	4.9	5.4	5.2	4.2	nd	0.2	nd	nd	nd
10	15.45	2,4-Dimethylphenol	4.8	4.4	4.8	4.6	3.9	0.2	0.3	0.2	0.1	0.1
11	15.53	2,3-Dimethylphenol	15.1	15.1	15.7	12.6	10.7	nd	0.6	nd	nd	nd
12	16.10	*p*-Ethylphenol	2.4	2.4	2.5	2.3	1.9	nd	0.1	nd	nd	nd
13	17.41	2,4,6-Trimethylphenol	4.7	4.7	5.2	4.7	4.0	0.2	0.2	0.2	0.2	nd
14	18.22	3-Ethyl-5-methylphenol	4.2	4.2	4.9	4.2	3.8	0.2	0.5	0.2	0.2	nd
15	18.55	3-Methyl-4-ethylphenol	19.6	19.6	21.6	21.6	18.6	nd	1.0	0.5	nd	nd
16	20.37	*o*-Allylphenol	11.3	12.7	11.8	8.9	8.5	nd	nd	nd	nd	nd
17	21.40	3-Methoxy-5-methylphenol	3.3	3.1	3.8	3.8	3.5	nd	0.2	nd	nd	nd
		Guaiacols	142.0	134.7	156.3	184.1	139.9	7.0	10.5	7.8	8.3	3.2
18	13.18	Guaiacol	31.8	29.2	32.8	42.4	30.7	3.2	3.8	3.3	3.8	1.4
19	16.40	6-Methylguaiacol	4.1	3.8	4.5	5.4	3.8	0.1	0.2	0.1	0.1	nd
20	16.89	*p*-Methylguaiacol	43.0	43.1	45.9	54.2	43.6	2.0	3.2	2.3	2.3	0.9
21	19.80	4-Ethylguaiacol	19.4	19.2	21.2	26.7	19.8	0.4	0.9	0.5	0.5	0.2
22	21.01	*p*-Vinylguaiacol	7.4	7.3	8.4	8.4	7.3	nd	0.3	nd	nd	nd
23	22.38	3-Allylguaiacol	3.2	3.0	3.9	4.1	3.1	0.2	nd	0.2	0.2	nd
24	22.72	*p*-Propylguaiacol	2.1	2.2	2.4	3.0	2.1	nd	nd	nd	nd	nd
25	23.78	5-Formylguaiacol	2.5	1.8	2.8	2.8	2.4	0.3	0.4	0.3	0.3	0.1
26	24.03	4-Propenylguaiacol	5.6	5.6	7.4	8.4	6.0	nd	nd	nd	nd	nd
27	25.38	cis-Isoeugenol	7.1	6.8	8.3	9.3	7.6	nd	0.1	nd	nd	nd
28	26.43	4-Acetylguaiacol	4.7	4.1	5.4	5.7	4.3	0.3	0.5	0.3	0.3	0.2
29	27.68	Guaiacylacetone	3.6	3.1	4.0	4.4	3.3	nd	0.4	0.3	0.3	nd
30	31.08	Homovanillic acid	4.3	3.1	4.9	5.3	3.7	0.4	0.6	0.4	0.4	0.3
31	46.91	Ethyl homovanillate	3.3	2.4	4.3	3.9	2.4	nd	nd	nd	nd	nd
		Catechols	37.3	31.1	44.8	50.2	34.3	16.4	18.7	17.0	16.7	9.9
32	17.12	Catechol	9.8	7.3	11.6	13.4	9.1	5.5	6.5	4.9	4.7	5.2
33	19.25	3-Methylcatechol	7.4	6.4	9.2	10.0	7.0	2.6	3.0	3.2	3.2	1.0
34	20.28	4-Methylcatechol	17.2	14.6	19.5	22.6	15.7	7.5	7.8	7.8	7.8	3.5
35	23.29	4-Ethylcatechol	3.0	2.8	4.5	4.3	2.5	0.7	1.4	1.1	1.0	0.2
		Others	12.7	14.9	15.3	6.9	5.7	0.0	0.0	0.0	0.0	0.0
36	11.58	Indene	2.5	3.3	2.3	nd	1.0	nd	nd	nd	nd	nd
37	16.61	Naphthalene	1.8	3.6	2.3	nd	nd	nd	nd	nd	nd	nd
38	17.96	2,3-Dihydrobenzofuran	1.6	1.6	1.5	nd	nd	nd	nd	nd	nd	nd
39	25.26	Acenaphthylene	1.7	2.3	2.2	nd	nd	nd	nd	nd	nd	nd
40	29.28	α-Amino-3′-hydroxy-4′-methoxyacetophenone	2.1	1.2	2.6	2.2	1.8	nd	nd	nd	nd	nd
41	44.61	Retene	1.7	1.7	2.3	2.5	1.8	nd	nd	nd	nd	nd
42	47.32	Methyl dehydroabietate	1.3	1.2	2.1	2.2	1.1	nd	nd	nd	nd	nd
Total identified compounds	312.3	300.6	338.5	353.0	264.3	28.7	37.9	30.6	29.4	14.6		
Total unidentified compounds	587.7	489.4	521.5	507.0	615.7	61.3	202.1	69.4	190.6	255.4		

RT: retention time, nd: not determined, and total unidentified = 1000-total identified – water content

the guaiacyl, and *p*-hydroxyphenyl groups. This may be due to the further degradation of the guaiacyl hydroxyl group into the catechol hydroxyl group, which is more favored than the degradation of the guaiacyl hydroxyl into the 4-hydroxyphenyl hydroxyl group, as shown in Figs. 6C and 7B (5) respectively. This confirms what was mentioned earlier. However, increasing the pyrolysis temperature decreases the concentration of catechols, as shown in Table 4. This might be the result of further degradation of the produced catechols. Ledesma et al. [21] reported catechol pyrolysis at a range of 973–1273 K, using CH, with a residence time of 0.4 s. According to their results, the decomposition of catechol started slowly at 873 K and then increased significantly at 973–1173 K. This is in agreement with the results presented here; catechols concentration decreased from 1.64 to 1.49 mmol/g when the temperature

Table 4
Concentration of hydroxyl groups determined by quantitative ^{31}P NMR spectroscopy of the raw lignin and the oil phases, using the method and peak assignments of Ben and Ragauskas [20].

Functional group		Integration region (ppm) [20]	Examples	Concentration in oil phase (mmol/g oil)					Conc. in lignin (mmol/g)
				900 K	980 K	1065 K	1150 K	1240 K	
Aliphatic OH		150.0–145.5	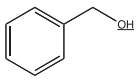	0.18	0.17	0.31	0.06	0.08	1.48
C_5 substituted condensed phenolic OH	β-5	144.7–142.8	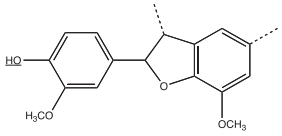	0.25	0.23	0.33	0.33	0.13	0.5
	4-O-5	142.8–141.7	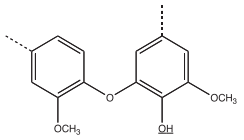	0.22	0.2	0.26	0.29	0.09	0.32
	5–5	141.7–140.2	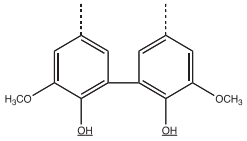	0.03	0.01	0.08	0.15	0.11	0.55
Guaiacyl phenolic OH		140.2–139.0	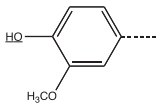	2.12	1.83	2.2	3.08	1.91	1.44
Catechol type OH		139.0–138.2	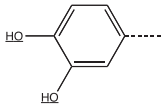	1.64	1.44	1.49	1.2	0.58	0.35
4-Hydroxy-phenyl OH		138.2–137.3	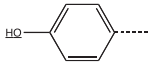	0.89	0.8	0.72	0.44	0.21	0.27
Acid–OH		136.6–133.6	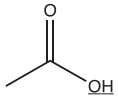	0.57	0.46	0.42	0.08	0	0.43

increased from 900 to 1065 K and decreased further when the temperature is increased to 1240 K. This confirms the occurrence of further degradation of the produced catechols. Many suggested mechanisms for this decomposition reported by Ledesma et al. [21].

The GC–MS analysis presented in Table 3 and the ^{31}P NMR analyses are in agreement that the most abundant identified groups are the guaiacols.

Since lignin does not interact well with EMW, the decomposition of aliphatic hydroxyl groups is more sensitive to the char wt% than to the nominal power setting. For instance, at the nominal power setting of 1.5 kW, the concentration of aliphatic hydroxyl groups was decreased from 0.18 to 0.06 mmol/g when the char wt% was increased from 20 to 40%. In addition, at the nominal power setting of 2.7 kW, it was decreased from 0.17 to 0.08 mmol/g, at the same char wt% concentrations, as illustrated in Table 4. In other words, the nominal power setting has a negligible effect on the degradation of aliphatic hydroxyl groups compared to the effect of char wt%.

3.4. Quantitative ^{13}C NMR analyses

Quantitative ^{13}C NMR spectroscopy was performed on every sample, for a total of six samples, which leads to further characterization for the functional groups in the oil phase as well as the raw material. Fig. 8 depicts the ^{13}C NMR spectra for the oil phases obtained at the conditions of 40 wt% of char and 1.5 kW of nominal power. Table 5 summarizes the integration for each of the analyzed samples.

Up to 80% of the identified carbons in the oil phase are aromatic carbons, which is logical according to the chemical structure of lignin. Each of the oil samples included concentration of aromatic C—O and C—C bonds is less than that in the raw-material. On the other hand, the number of aromatic C—H bonds in the oil phase was more than that in the raw material for all the investigated conditions.

Together, the ^{13}C NMR and ^{31}P NMR results support the degradation pathways proposed above. The decreased number of C—O aromatic bonds after the MW-P may be due to the decomposition of the ether bond during MW-P, as illustrated in Fig. 7. In addition, the further decomposition of the *o*-hydroxyphenoxymethyl radical could have contributed to the decrease, as in Fig. 7B((5), (6)), although this is not favored. The decreased number of C_{arom}—C bonds may be due to the degradation of the carboxyl hydroxyl group and the C5 substituted/condensed phenolic hydroxyl groups, as in β-5 and 5-5 bonds, as presented in Figs. 6B and and 7, respectively. On the other hand, the increased number of C_{arom}—H bonds may be due to the decomposition of the ether bond during pyrolysis and the degradation of C_{arom}—C bonds, as illustrated in Fig. 7. In addition, the changes in the number of C—H bond are interrelated

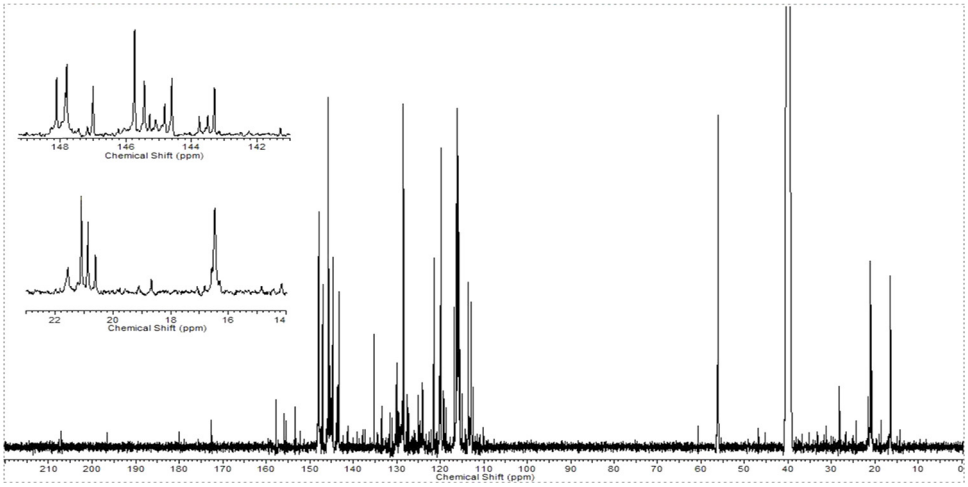

Fig. 8. Quantitative ^{13}C NMR spectra for the oil phase obtained at the conditions of 40 wt% of char and 1.5 kW of nominal power.

Table 5
Concentration of different types of carbon atoms measured by quantitative ^{13}C NMR spectroscopy of the raw lignin and the obtained oil phases, using the method and peak assignments of Ben and Ragauskas [20].

Functional group		Integration region (ppm) [20]	Examples	Concentration in oil phase (C mol%)					Conc. in lignin (C mol%)
				900 K	980 K	1065 K	1150 K	1240 K	
Carbonyl or carboxyl		215.0–166.5	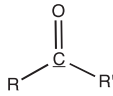	0.11	0.06	0.0	0.0	0.0	0
Aromatic C—O		166.5–142.0	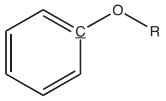	23.5	23.9	26.1	28.4	25.4	32.18
Aromatic C—C		142.0–125.0	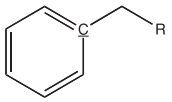	10.8	11.6	11.7	6.2	8.3	21.05
Aromatic C—H		125.0–95.8	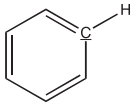	46.1	42.2	39.9	42.2	43.0	21.21
Aliphatic C—O		95.8–60.8	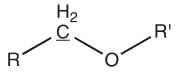	0.0	0.0	0.0	0.1	0.0	0
Methoxyl-aromatic		60.8–55.2	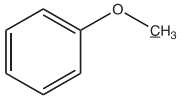	9.5	10.4	11.5	12.3	11.1	22.38
Aliphatic C—C	Total	55.2–0.0	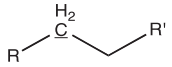	10.0	12.0	10.7	10.8	12.1	3.19
	Methyl – aromatic	21.6–19.1	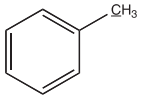	4.3	6.0	5.6	5.4	5.7	0
	Methyl – aromatic ortho to a hydroxyl or methoxyl group	16.8–15.4	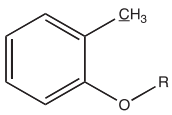	5.4	4.3	4.2	4.3	4.6	0

with the modifications in the C—C and C—O bonds. As a result, when the percentage of C—O and/or C—C bonds was reduced, the percentage of C—H bonds increased, as shown in Table 5. The increased number of C_{methyl}—C_{arom} bonds may be due to the cleavage of the aliphatic hydroxyl groups, as shown in Fig. 6A.

4. Conclusions

A detailed compositional analysis and structural investigation of bio-oil produced via microwave pyrolysis (MW-P) of kraft lignin was accomplished. MW-P was performed at different conditions of weight% of a microwave-absorber (char, 20–40%) and nominal power setting (1.5–2.7 kW). GC–MS and GC–FID analyses were implemented on the oil and aqueous phases, and ^{31}P and ^{13}C NMR analyses were performed on the oil phase and the raw material. One of the main conclusions of this work includes the greater effect of char wt% than power setting on the heating rate. Increasing the pyrolysis final temperature, i.e., increasing of the heating rate; augmented the total obtained liquid yield; however, beneficial depending on the composition of the liquid phases. The identified concentrations of chemical compounds obtained in the oil phase were 264–353 mg/g in contrast to 15–38 mg/g identified in the aqueous phase. Nonetheless, a concentration of 490–616 mg/g of the oil phase could not be identified, due to the limitations of the GC–MS. Therefore, a GC–MS analysis is inadequate to provide a detailed structure of the pyrolysis liquids. On the basis of ^{31}P and ^{13}C NMR analyses, up to 80% of the carbon atoms in the oil phase were aromatic carbons. The concentration of aliphatic hydroxyl groups in the raw material was significantly decreased by the MW-P. This was attributed to water forming during the thermal degradation of the lignin network. The decreased concentrations of C5 substituted/condensed phenolic hydroxyl groups after MW-P could be contributed to the increase in the concentrations of guaiacyl, *p*-hydroxyphenyl, and catechol hydroxyl groups.

The optimum condition obtained from this investigation was used in a kinetic modeling to simulate the MW-P products, solid, liquid, and gas, as well as the extracted chemicals using lumped approach, Farag et al. [5]. Furthermore, a developed method using switchable hydrophilicity solvents was documented to extract phenols from the obtained oil phase, Fu et al. [18].

Acknowledgements

The authors thank Mr. Yazid Belkhir and Mr. Robert Delisle (Technicians at Ecole Polytechnique Montreal) for their assistance in the experimental setup, and Dr. Levent Erdogan (Electrical Engineering Department, Ecole Polytechnique Montreal) and Ms. Mai Attia (Student at UQAM University Montreal) for their assistance in this work. In addition, the authors are grateful for the financial and technical support from Lignoworks NSERC Strategic Network (lignoworks.ca), and providing the raw material from FPInnovations, Montreal, Quebec, Canada.

References

[1] P.J. de Wild, W.J.J. Huijgen, H.J. Heeres, Pyrolysis of wheat straw-derived Organosolv lignin, J. Anal. Appl. Pyrol. 93 (0) (2012) 95–103.
[2] W. Mu, et al., Lignin pyrolysis components and upgrading-technology review, BioEnergy Res. (2013) 1–22.
[3] J. Zakzeski, et al., The catalytic valorization of lignin for the production of renewable chemicals, Chem. Rev. 110 (6) (2010) 3552–3599.
[4] J. Kibet, L. Khachatryan, B. Dellinger, Molecular products and radicals from pyrolysis of lignin, Environ. Sci. Technol. 46 (23) (2012) 12994–13001.
[5] S. Farag, L. Kouisni, J. Chaouki, Lumped approach in kinetic modeling of microwave pyrolysis of kraft lignin, Energy Fuels 28 (2) (2014) 1406–1417.
[6] J. Doucet, et al., Distributed microwave pyrolysis of domestic waste, Waste Biomass Valoriz. (2013) 1–10.
[7] S. Farag, et al., Temperature profile prediction within selected materials heated by microwaves at 2.45 GHz, Appl. Therm. Eng. 36 (0) (2012) 360–369.
[8] Y. Zheng, D. Chen, X. Zhu, Aromatic hydrocarbon production by the online catalytic cracking of lignin fast pyrolysis vapors using Mo2N/(−Al_2O_3, J. Anal. Appl. Pyrol. 104 (0) (2013) 514–520.
[9] R. Lou, S.-b. Wu, G.-j. Lv, Effect of conditions on fast pyrolysis of bamboo lignin, J. Anal. Appl. Pyrol. 89 (2) (2010) 191–196.
[10] G. Jiang, D.J. Nowakowski, A.V. Bridgwater, Effect of the temperature on the composition of lignin pyrolysis products, Energy Fuels 24 (8) (2010) 4470–4475.
[11] H.S. Choi, D. Meier, Fast pyrolysis of kraft lignin – vapor cracking over various fixed-bed catalysts, J. Anal. Appl. Pyrol. 100 (0) (2013) 207–212.
[12] M. Zhang, et al., Pyrolysis of lignin extracted from prairie cordgrass: aspen, and kraft lignin by Py-GC/MS and TGA/FTIR, J. Anal. Appl. Pyrol. 98 (0) (2012) 65–71.
[13] Z. Luo, S. Wang, X. Guo, Selective pyrolysis of Organosolv lignin over zeolites with product analysis by TG-FTIR, J. Anal. Appl. Pyrol. 95 (0) (2012) 112–117.
[14] A. Undri, et al., Efficient disposal of waste polyolefins through microwave assisted pyrolysis, Fuel 116 (0) (2014) 662–671.
[15] A. Undri, et al., Reverse polymerization of waste polystyrene through microwave assisted pyrolysis, J. Anal. Appl. Pyrol. 105 (0) (2014) 35–42.
[16] A. Domínguez, et al., Production of bio-fuels by high temperature pyrolysis of sewage sludge using conventional and microwave heating, Bioresour. Technol. 97 (10) (2006) 1185–1193.
[17] S. Farag, J. Chaouki, A modified microwave thermogravimetric-analyzer for kinetic purposes, Appl. Therm. Eng. (2014) (submitted for publication).
[18] D. Fu, et al., Extraction of phenols from lignin microwave-pyrolysis oil using a switchable hydrophilicity solvent, Bioresour. Technol. 154 (0) (2014) 101–108.
[19] A. Granata, D.S. Argyropoulos, 2-Chloro-4,4,5,5-tetramethyl-1,3,2-dioxaphospholane, a reagent for the accurate determination of the uncondensed and condensed phenolic moieties in lignins, J. Agric. Food Chem. 43 (6) (1995) 1538–1544.
[20] H. Ben, A.J. Ragauskas, NMR characterization of pyrolysis oils from kraft lignin, Energy Fuels 25 (5) (2011) 2322–2332.
[21] E.B. Ledesma, et al., An experimental study on the thermal decomposition of catechol, Proceedings of the Combustion Institute 29 (2) (2002) 2299–2306.